Moments of the Neutron Charge Form Factor and the $N \rightarrow \Delta$ Quadrupole Transition

P. Grabmayr* and A. J. Buchmann[†]

Physikalisches Institut, Universität Tübingen, D-72076 Tübingen, Germany
(Received 28 March 2000; revised manuscript received 7 November 2000)

Recent data allow a new parametrization of the neutron charge form factor G_E^n. A parameter-free quark-model relation between G_E^n and the $N \rightarrow \Delta$ quadrupole form factor $G_{C2}^{N \rightarrow \Delta}$ is used to predict $G_{C2}^{N \rightarrow \Delta}$ from G_E^n data. In particular, $\langle r_n^2 \rangle$ is related to $N \rightarrow \Delta$ quadrupole moment $\mathcal{Q}_{N \rightarrow \Delta}$, while $\langle r_n^4 \rangle$ connects to the $N \rightarrow \Delta$ quadrupole transition radius $\langle r_{N \rightarrow \Delta}^2 \rangle$. From the latter we derive an experimental value for the charge radius of the light constituent quarks $r_{\gamma q} = 0.8$ fm. Finally, the $C2/M1$ ratio in pion electroproduction is predicted from the elastic neutron form factor data.

Intrinsic nucleon structure.—The nucleon is a complicated many-particle system composed of valence quarks, which carry the quantum numbers, and nonvalence quark degrees of freedom, which describe the cloud of quark-antiquark ($q\bar{q}$) pairs and gluons. The constituent quark model with two-body exchange currents describes both these aspects of nucleon structure [1]. One-body currents describe the interaction of the photon with one valence quark at a time. Two-body exchange currents are connected with the exchange particles (gluons, pions) and with $q\bar{q}$ pairs [see Figs. 1(b)–1(d)]. Nucleon properties which are dominated by two-body exchange currents show their common dynamical origin in analytical interrelations.

In this paper, a quark model relation between the neutron charge form factor G_E^n and the quadrupole transition form factor $G_{C2}^{N \rightarrow \Delta}$ is used together with a parametrization of new G_E^n data to predict $G_{C2}^{N \rightarrow \Delta}$ and the $C2/M1$ ratio usually measured by pion electroproduction. The spin-isospin dependence of the two-body charge operator $\rho_{[2]}$, e.g., for the gluon, can be written schematically as

$$\rho_{[2]} \approx \sum_{i \neq j} e_i \left[\boldsymbol{\sigma}_i \cdot \boldsymbol{\sigma}_j Y^0(\mathbf{q}) - \frac{\sqrt{6}}{2} \{ [\boldsymbol{\sigma}_i \times \boldsymbol{\sigma}_j]^2 \times Y^2(\mathbf{q}) \}^0 \right], \quad (1)$$

where $\mathbf{q}$ is the three-momentum transfer and e_i and $\boldsymbol{\sigma}_i$ are, respectively, the quark charge and spin. Explicit expressions can be found in Ref. [1].

As a result of (i) the dominance of $\rho_{[2]}$ [1,2] and of (ii) the spin-isospin structure in $\rho_{[2]}$ and in the N and Δ wave functions, a connection between the neutron charge form factor $G_E^n(\mathbf{q}^2)$ and the $N \rightarrow \Delta$ quadrupole transition form factor $G_{C2}^{N \rightarrow \Delta}(\mathbf{q}^2)$ emerges [3] as follows:

$$G_{C2}^{N \rightarrow \Delta}(\mathbf{q}^2) = -\frac{3\sqrt{2}}{\mathbf{q}^2} G_E^n(\mathbf{q}^2). \quad (2)$$

The derivation is independent of the spatial part of the quark wave functions and holds irrespective of whether gluon or pion exchange or both are employed. One-body

contributions to G_E^n and $G_{C2}^{N \rightarrow \Delta}$ arise only through excited-state admixtures which amount to less than 20% of the empirical values if a quark core radius consistent with the excitation spectrum [2,4] is used. Three-body corrections are estimated to contribute less than 30% of the two-body currents using a QCD parametrization [5] and a large $1/N_c$ approach [6]. These approaches also show the dominance of the two-body exchange currents for both observables.

The dominance of nonvalence quark degrees of freedom in G_E^n and $G_{C2}^{N \rightarrow \Delta}$ is not specific to this quark model. Also chiral approaches, e.g., the Skyrme model [7], the σ model [8], the Nambu-Jona-Lasinio model [9], and the chiral soliton model with quarks [10] predict that the neutron charge radius $\langle r_n^2 \rangle$ and $\mathcal{Q}_{N \rightarrow \Delta}$, the transition quadrupole moment, are dominated by nonvalence quark degrees of freedom. In these models, the valence quark contribution to $\langle r_n^2 \rangle$ and $\mathcal{Q}_{N \rightarrow \Delta}$ is comparatively small. The quark model, the chiral approaches [11], and chiral perturbation theory [12] have the same underlying group theoretical structure, i.e., spin-isospin symmetry. Equation (2) has been derived within the constituent quark model for the case of dominance of two-body operators. However, a larger range of validity is conjectured because of stringent constraints on allowed operator structures in Eq. (1) due to the scalar nature of the charge operator and the spin-isospin symmetry of the N and Δ wave functions.

For further interpretation of the new G_E^n parametrization we rely on explicit expressions for the lowest moments of G_E^n and $G_{C2}^{N \rightarrow \Delta}$ calculated in the quark model with two-body currents. In this model [1], the neutron charge radius can be expressed in terms of the empirical N-Δ mass splitting and the quark core radius b
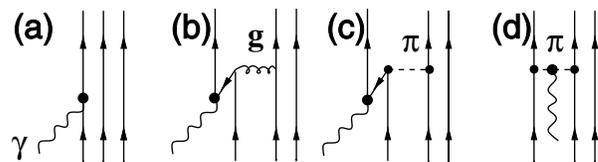

FIG. 1. Feynman diagrams of the four-vector current J^μ with photon coupling to (a) one-body current $J_{[1]}^\mu$ and to (b)–(d) two-body gluon and pion exchange currents $J_{[2]}^\mu$.

$$\langle r_n^2 \rangle = -b^2 \frac{M_\Delta - M_N}{M_N}. \qquad (3)$$

Inserting the experimental neutron charge radius $\langle r_n^2 \rangle = -0.113$ fm^2 [13] and the experimental N-Δ mass splitting into Eq. (3) one obtains $b = 0.60$ fm for the quark core radius, which measures the spatial extent of the valence quark wave function. A related quantity of interest is the slope of $G_{C2}^{N \to \Delta}$ at $\mathbf{q}^2 = 0$, which is given by [2,3]

$$\langle r_{N \to \Delta}^2 \rangle = \frac{11}{20} b^2 + r_{\gamma q}^2, \qquad (4)$$

where $r_{\gamma q}^2$ is the charge radius of the constituent quark. In the same model we find $G_{M1}^{N \to \Delta}(\mathbf{q}^2) = -\sqrt{2}\, G_M^n(\mathbf{q}^2)$.

Moments of form factors.—First, at low momentum transfers $Q^2 = -q_\mu^2$ any form factor (here G_E^n) can be expanded into a Taylor series

$$G_E^n(Q^2) = G_E^n(0) + \left. \frac{dG_E^n}{dQ^2} \right|_{Q^2=0}$$
$$\times\, Q^2 + \frac{1}{2} \left. \frac{d^2 G_E^n}{(dQ^2)^2} \right|_{Q^2=0} Q^4 + \cdots. \qquad (5)$$

Second, in the Breit frame ($Q^2 = \mathbf{q}^2$) the form factor G_E^n is related to the spatial charge distribution $\rho(r)$ through the Fourier transform as

$$G_E^n(Q^2) = \int_0^\infty \rho(r) e^{-i\mathbf{q}\cdot\mathbf{r}}\, d\mathbf{r}$$
$$= 4\pi \int_0^\infty \rho(r) \frac{\sin qr}{qr} r^2\, dr. \qquad (6)$$

A series expansion of $\sin(qr)$ leads to the well known relation between the derivatives of the electric form factor and the radial moments of the charge distribution

$$G_E^{n'}(0) \equiv \left. \frac{dG_E^n}{dQ^2} \right|_{Q^2=0} = -\frac{\langle r_n^2 \rangle}{6} = -\frac{a\mu_n}{4M_n^2}, \qquad (7)$$

$$G_E^{n''}(0) \equiv \left. \frac{d^2 G_E^n}{(dQ^2)^2} \right|_{Q^2=0} = \frac{\langle r_n^4 \rangle}{60} = \frac{a\mu_n}{4M_n^2}\left[\frac{4}{\Lambda^2} + \frac{d}{2M_n^2} \right], \qquad (8)$$

$$\mathcal{R} \equiv \frac{G_E^{n''}(0)}{G_E^{n'}(0)} = -\frac{1}{10}\frac{\langle r_n^4 \rangle}{\langle r_n^2 \rangle} = -\left[\frac{4}{\Lambda^2} + \frac{d}{2M_n^2} \right]. \qquad (9)$$

The right-hand sides are obtained by taking the first and second derivative of the common parametrization of G_E^n:

$$G_E^n(Q^2) = -\mu_n \frac{a\tau}{1+d\tau} G_D(Q^2) \qquad (10)$$

with $G_D(Q^2) = 1/(1 + Q^2/\Lambda^2)^2$, $\Lambda^2 = 0.71 (\text{GeV}/c)^2$, and $\tau = Q^2/4M_n^2$ (see Refs. [14,15]), and with μ_n the neutron magnetic moment. This simple parametrization guarantees the proper behavior of G_E^n at $Q^2 = 0$ (zero net charge) and at $Q^2 \to \infty$ (quark counting rules).

Similarly, the low momentum expansion of $G_{C2}^{N \to \Delta}$ can be written as

$$G_{C2}^{N \to \Delta}(Q^2) = \mathcal{Q}_{N \to \Delta}\left(1 - \frac{\langle r_{N \to \Delta}^2 \rangle}{6} Q^2 + \cdots \right). \qquad (11)$$

Referring to the connection between $G_{C2}^{N \to \Delta}$ and G_E^n [Eq. (2)] and equating the respective coefficients of Eqs. (11) and (5) one finds with the help of Eqs. (7)–(9)

$$\mathcal{Q}_{N \to \Delta} = \frac{\langle r_n^2 \rangle}{\sqrt{2}} = \frac{3a}{2\sqrt{2}}\frac{\mu_n}{M_n^2}. \qquad (12)$$

$$\langle r_{N \to \Delta}^2 \rangle = \frac{6}{20\sqrt{2}}\frac{\langle r_n^4 \rangle}{\mathcal{Q}_{N \to \Delta}} = \frac{3}{10}\frac{\langle r_n^4 \rangle}{\langle r_n^2 \rangle} = -3\mathcal{R}. \qquad (13)$$

New G_E^n data and fits.—There has recently been increased interest in the neutron electric form factor itself as a testing ground for nucleon models. Furthermore, G_E^n must be known accurately in order to analyze for example parity violation and $N \to \Delta$ transition experiments. The previous evaluation by Platchkov *et al.* [15] of elastic electron-deuteron scattering data is model dependent because the analysis relies heavily on the deuteron wave function when subtracting all magnetic form factors and the charge contribution of the proton in order to isolate G_E^n from the measured cross sections. The analysis employing the Paris potential was then considered as the most reliable [15]; other choices for the NN potential yielded values for G_E^n differing up to 100%. The results were parametrized using Eq. (10) with the two parameters fitted to $a = 1.25$ and $d = 18.3$. An earlier analysis [14] obtained the values $a = 1.0$ and $d = 10.7$, respectively.

In modern double-polarization experiments, where the ratio of G_E^n/G_M^n is measured in quasifree kinematics, the NN-potential dependence is greatly reduced. The remaining uncertainty resides mainly in the corrections for final state interaction (FSI) and to a lesser extent for meson exchange currents (MEC) between the nucleons. Recent experiments have been performed at Bates, Amsterdam, and Mainz by using polarized electrons scattering either from unpolarized deuterium and measuring the recoil polarization of the neutron [16–19] or by measuring helicity dependences on polarized ^{3}He [20–23]. Only four of these data with sufficient statistical and systematic accuracy have been selected (Table I) and are displayed in Fig. 2. A further selection criterium was the coincident detection of neutrons and scattered electrons which enables a check on the quasifree scattering mechanism.

TABLE I. G_E^n data resulting from recent experiments are selected and are listed with statistical (Δ_{stat}) and total ($\Delta_{\text{tot}} = \Delta_{\text{stat}} + \Delta_{\text{syst}}$) errors. The $\langle r_n^2 \rangle$ values from electron-neutron scattering are given in the last line.

$Q^{2\,a}$	G_E^n	Δ_{stat}	Δ_{tot}	Ref.
0.15	0.0480	0.0065	0.0118	[16]
0.21	0.0660	0.0150	0.0190	[17]
0.34	0.0611	0.0069	0.0129	[18]
0.67	0.0520	0.0110	0.0160	[20]
	$\langle r_n^2 \rangle$ $^{\text{b}}$	Δ_{stat} $^{\text{b}}$	Δ_{tot} $^{\text{b}}$	
0.0	-0.113	0.0026	0.0060	[13]

$^{\text{a}}$In units of $(\text{GeV}/c)^2$.
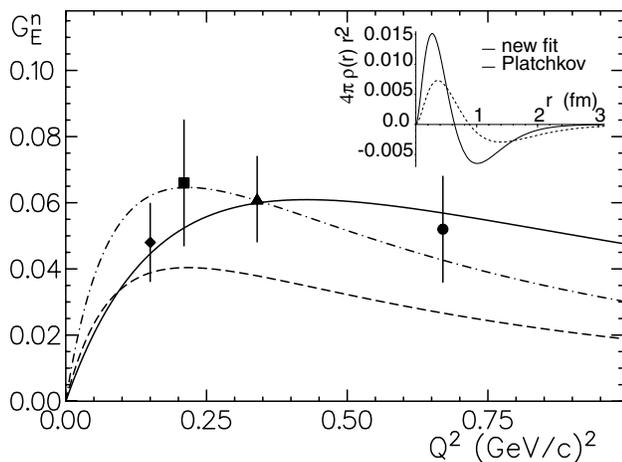$^{\text{b}}$In units of fm^2.

FIG. 2. Recent measurements of G_E^n are given by the full points (see Table I). The Platchkov parametrization [15] (dashed line) is shown together with a fit to the new data without (dot-dashed line) and with (full line) inclusion of $\langle r_n^2 \rangle$ from Ref. [13]. The inset shows the neutron charge distributions resulting from the new (full line) and the Platchkov (dashed line) parametrizations.

The three deuteron data [16–18] rely on corrections based on calculations by Arenhövel [24]. Corrections for the ^{3}He data at $Q^2 = 0.35$ (GeV/c)^2 [21,22] are expected to be quite large. Therefore, these ^{3}He data were not considered in the present fits. Note however, that the correction at $Q^2 = 0.67$ (GeV/c)^2 is estimated to amount to only 10%, which has not been applied to the data but is included in the systematical error [20].

Statistical errors are given in column 3 of Table I. The sum $\Delta_{\rm tot} = \Delta_{\rm stat} + \Delta_{\rm syst}$ of statistical and systematical errors is shown separately in column 4. In view of the discussion above, we will use $\Delta_{\rm tot}$ in this analysis. The data are shown in Fig. 2 together with the (dashed line) curve based on the Platchkov parametrization with the Paris potential [15]. We note that the new data lie significantly above the previous evaluation.

Parameters a and d of Eq. (10) have been obtained by a "downhill simplex" fit using the four data points from quasifree scattering and the $\langle r_n^2 \rangle$ value [13] obtained from thermal neutron electron scattering. The results and their standard deviations due to the fit with $\Delta_{\rm tot}$ are compiled in Table II, together with the total χ^2. For reference, the parametrizations of Galster [14] and Platchkov [15] are listed in the last two lines of Table II showing large values for χ^2. The first two lines of Table II present the fitting results for different conditions as marked in the first column. From Eq. (7) it is evident that parameter a is determined exclusively by $\langle r_n^2 \rangle$, which leads to a strong reduction of Δa when $\langle r_n^2 \rangle$ is included in the fit. The result including this constraint (line 2 of Table II) is regarded as the most reliable, considering the present status of the database. It is represented by the full curve in Fig. 2. The influence of omitting the $\langle r_n^2 \rangle$ datum in the fit (line 1 of Table II) is shown by the dot-dashed line. From this fit a neutron charge radius of $\langle r_n^2 \rangle = -0.178(27)$ fm^2 would be deduced which is ruled out by the analysis of Ref. [13]. Despite its large uncertainty the parameter d is much smaller than previously assumed [15] which is reflected by smaller values for $G_E^{n\prime\prime}(0)$ and $\mathcal{R}$ as shown in the last two columns.

With the present fit the inverse Fourier transformation of Eq. (6) leads to a neutron charge distribution (full line in Fig. 2 inset) quite different from the previous results (Ref. [15], dashed line), and thus to different moments. The inner region of positive contributions is compressed and the zero crossing point is shifted by about 0.2 fm towards the center, compared to the old distribution. Note that the new zero coincides with the value for the quark core radius b derived from Eq. (3).

A better determination of parameter d, which is crucial for the second derivative of G_E^n, calls for additional data at high Q^2 where corrections for FSI and MEC are less important. Although the cross sections decrease with Q^2, a statistical error $\Delta_{\rm stat} = 5\%$ is attainable and the chosen error $\Delta_{\rm tot} = 10\%$ seems to be realistic. Simple values for G_E^n have been assumed to demonstrate possible variations

TABLE II. Parameters a and d from fits to the data of Table I together with χ^2 are shown in the first two lines; values for $G_E^{n\prime\prime}(0)$ [Eq. (8)] and the ratio $\mathcal{R}$ [Eq. (9)] are also given. The next three lines contain results where one additional fictitious data point with $\Delta_{\rm tot} = 10\%$ at $Q^2 = 0.9$ (GeV/c)^2 is included in the data set for which the assumed G_E^n value is given in column 1. For reference the results using the parameters of Refs. [14] and [15] are shown in the last two lines.

Comments	$a \pm \Delta a$	$d \pm \Delta d$	χ^2	$G_E^{n\prime\prime}$ [a]	$\mathcal{R}$ [b]
[c]	1.415 (0.213)	9.06 (3.30)	0.09	−8.26	−10.77
	0.898 (0.044)	2.74 (1.99)	0.63	−3.50	−7.19
$G_E^n = 0.04$	0.903 (0.040)	4.30 (0.77)	1.30	−3.95	−8.07
$G_E^n = 0.05$	0.898 (0.041)	2.78 (0.66)	0.63	−3.51	−7.21
$G_E^n = 0.06$	0.894 (0.040)	1.75 (0.61)	1.07	−3.21	−6.63
Ref. [14]	1.00 ($\cdots$)	10.70 ($\cdots$)	10.53	−6.35	−11.69
Ref. [15]	1.25 ($\cdots$)	18.30 ($\cdots$)	62.65	−10.83	−16.00

[a]In units of (GeV/c)$^{-4}$.
[b]In units of (GeV/c)$^{-2}$.
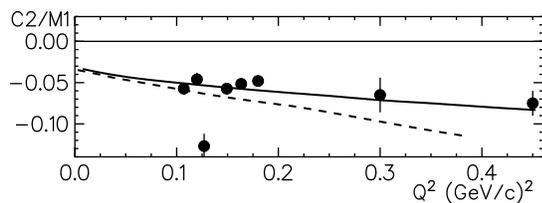[c]$\langle r_n^2 \rangle$ datum omitted.

FIG. 3. Ratio $C2/M1$ from the present fit to G_E^n (solid line) and from calculations of Ref. [3] (dashed line) in comparison with experimental results taken from Refs. [25,26].

of d. In Table II we present three more fits each with one fictitious data point added at $Q^2 = 0.9$ $(\text{GeV}/c)^2$. The additional datum at $Q^2 = 0.9$ $(\text{GeV}/c)^2$ reduces Δd by a factor 3. Because the highest data point at $Q^2 = 0.6$ $(\text{GeV}/c)^2$ does not include any FSI correction, a further decrease of parameter d towards a value of 2 seems likely.

Results.—The fits of G_E^n and, in particular, the first extraction of the fourth moment $\langle r_n^4 \rangle = -0.32(8)$ fm^4 permit a prediction for $\langle r_{N\to\Delta}^2 \rangle = 0.84(21)$ fm^2 where the error is determined only through Δd [see Eq. (9)]; with the additional sixth data point the error of $\langle r_{N\to\Delta}^2 \rangle$ would be reduced to 0.07 fm^2. The variation of d and thus $\mathcal{R}$ with the sixth data point is indicative of a possible 10% change of $\langle r_{N\to\Delta}^2 \rangle$. By the use of Eq. (4) and a quark core radius $b = 0.6$ fm we obtain for the charge radius of the light constituent quarks of $r_{\gamma q}^2 = 0.64$ fm^2. This value is somewhat larger than the value derived from the vector dominance model, which would give $r_{\gamma q}^2 = 6/m_\rho^2 = 0.4$ fm^2.

Furthermore, the low momentum expansion [Eq. (11)] can be expressed as $G_{C2}^{N\to\Delta}(Q^2) \approx -0.08(1 - 3.6 \cdot Q^2)$ fm^2 when substituting the parameters a and $\mathcal{R}$ by numbers from the new fit. This is in reasonable agreement with the direct estimates of the constituent quark model [2].

Finally, in the quark model with two-body exchange currents the $C2/M1$ ratio can be expressed as a ratio of the elastic neutron charge and magnetic form factors [3]

$$\frac{C2}{M1} = M_N \frac{\sqrt{\mathbf{q}^2}}{6} \frac{G_{C2}^{N\to\Delta}(\mathbf{q}^2)}{G_{M1}^{N\to\Delta}(\mathbf{q}^2)} = \frac{M_N}{2\sqrt{\mathbf{q}^2}} \frac{G_E^n(\mathbf{q}^2)}{G_M^n(\mathbf{q}^2)}. \quad (14)$$

Using $G_M^n = \mu_n G_D$ we compare the predictions of Eq. (14) with the direct measurements [25,26] of the $C2/M1$ ratio in pion electroproduction. Starting from the new parametrization of G_E^n we find the ratio in the range of -0.03 to -0.08 (full line in Fig. 3). The data [25,26] in general are in the range of -0.046 to -0.06. The agreement is surprising, which hints at the general validity of the relation between $G_E^n G_M^n$ and $C2/M1$ [Eq. (14)]. A constituent quark model calculation [3] of this ratio (dashed line) comes lower than the parametrization. Differences between this calculation and the $C2/M1$ data may be explained by possible background amplitudes contributing to the $N \to \Delta$ transition. Other constituent quark model calculations based on one-body currents alone, e.g.,

Ref. [27], predict much smaller ratios, mostly in the range of -0.005 to -0.02 (see also references in [25]).

In summary, we have performed a fit to the most reliable data for G_E^n below $Q^2 < 1$ $(\text{GeV}/c)^2$. We use the obtained parametrization in combination with relations originally derived in the constituent quark model to predict the quadrupole transition form factor $G_{C2}^{N\to\Delta}$ and its leading moments $\mathcal{Q}_{N\to\Delta}$ and $\langle r_{N\to\Delta}^2 \rangle$. Equation (2) provides a determination of $C2/M1$ through the elastic neutron form factors which agrees well with $C2/M1$ data from pion electroproduction experiments.

*Email address: grabmayr@pit.physik.uni-tuebingen.de
†Email address: alfons.buchmann@uni-tuebingen.de

[1] A. Buchmann, E. Hernández, and K. Yazaki, Phys. Lett. B **269**, 35 (1991); Nucl. Phys. **A569**, 661 (1994).
[2] A. J. Buchmann, E. Hernández, and A. Faessler, Phys. Rev. C **55**, 448 (1997); A. J. Buchmann, Z. Naturforsch. A **52**, 877 (1997).
[3] A. J. Buchmann, Nucl. Phys. **A670**, 174c (2000).
[4] M. M. Giannini, Rep. Prog. Phys. **54**, 453 (1990).
[5] G. Dillon and G. Morpurgo, Phys. Lett. B **448**, 107 (1999).
[6] A. J. Buchmann and R. F. Lebed, Phys. Rev. D **62**, 096005 (2000).
[7] A. Wirzba and W. Weise, Phys. Lett. B **188**, 7 (1987); J. Kroll and B. Schwesinger, Phys. Lett. B **334**, 287 (1994).
[8] M. Fiolhais *et al.,* Phys. Lett. B **373**, 229 (1996).
[9] C. Christov *et al.,* Prog. Part. Nucl. Phys. **37**, 91 (1996).
[10] T. Cohen and W. Broniowski, Phys. Rev. D **34**, 3472 (1986).
[11] A. V. Manohar, Nucl. Phys. **B248**, 19 (1984).
[12] R. F. Lebed, Nucl. Phys. **B430**, 295 (1994).
[13] S. Kopecky *et al.,* Phys. Rev. Lett. **74**, 2427 (1995).
[14] S. Galster *et al.,* Nucl. Phys. **B32**, 221 (1971).
[15] S. Platchkov *et al.,* Nucl. Phys. **A570**, 740 (1990).
[16] C. Herberg *et al.,* Eur. Phys. J. A **5**, 131 (1999).
[17] I. Passchier *et al.,* Phys. Rev. Lett. **82**, 4988 (1999).
[18] M. Ostrick *et al.,* Phys. Rev. Lett. **83**, 276 (1999).
[19] T. Eden *et al.,* Phys. Rev. C **50**, R1749 (1994).
[20] D. Rohe *et al.,* Phys. Rev. Lett. **83**, 4257 (1999).
[21] M. Meyerhoff *et al.,* Phys. Lett. B **327**, 201 (1994).
[22] J. Becker *et al.,* Eur. Phys. J. A **5**, 329 (1999).
[23] C. Jones-Woodward *et al.,* Phys. Rev. C **44**, R571 (1991); A. K. Thompson *et al.,* Phys. Rev. Lett. **68**, 2901 (1992).
[24] H. Arenhövel, Z. Phys. A **331**, 123 (1988).
[25] P. Bartsch *et al.,* in *Proceedings of Baryons' 98, Bonn, Germany,* edited by D. W. Menze and B. Metsch (World Scientific, Singapore, 1999), p. 757; R. Gothe, *ibid.,* p. 394; P. Stoler, *ibid.,* p. 408; M. O. Distler, *ibid.,* p. 753; R. Gothe, in *Proceedings of N*2000, Newport News, VA* (World Scientific, Singapore, 2001).
[26] R. Siddle *et al.,* Nucl. Phys. **B35**, 93 (1971); J. C. Alder *et al.,* Nucl. Phys. **B46**, 573 (1972).
[27] S. Capstick and G. Karl, Phys. Rev. D **41**, 2767 (1990).